

# Optical Engineering

[SPIDigitalLibrary.org/oe](http://SPIDigitalLibrary.org/oe)

## **Design and development of telescope control system and software for the 50/80 cm Schmidt telescope**

Tripurari S. Kumar  
Ravi N. Banavar

# Design and development of telescope control system and software for the 50/80 cm Schmidt telescope

**Tripurari S. Kumar**

Indian Institute of Technology Bombay  
Systems and Control Engineering  
Mumbai 400076, India  
and

Aryabhata Research Institute of Observational  
Sciences

Electronics Section  
Nainital 263129, India  
E-mail: [kumar@sc.iitb.ac.in](mailto:kumar@sc.iitb.ac.in)

**Ravi N. Banavar**

Indian Institute of Technology Bombay  
Systems and Control Engineering  
Mumbai 400076, India

**Abstract.** We describe the details of telescope control system design for the 50/80 cm Schmidt telescope at the Aryabhata Research Institute of Observational Sciences. The overall control hardware architecture features a distributed network of microcontrollers over controller area network for interfacing the feedback elements and controlling the actuators. The main part of the hardware is a controller whose final objective is to provide position control with 10 arcsec accuracy and velocity control with 1 arcsec/s accuracy. For modeling and simulation, the telescope parameters were experimentally determined. A linear proportional integral (PI) controller was designed for controlling the twin-motor drive mechanism of the telescope axes. The twin-motor drive is provided with differential torque for backlash-free motion reversal. This controller is able to maintain negligible rms errors at all velocities. At higher speeds over 2 deg/s, the PI controller performs with peak errors less than 1%. Whereas at fine speeds, depending upon the preload on bearings, limit cycles are exhibited due to nonlinear friction posing control related problems. We observed that the effect of nonlinear friction dynamics can be reduced by reducing the preload on the drive bearings and the peak errors at fine speeds using a linear controller can be maintained within 25%. © 2013 Society of Photo-Optical Instrumentation Engineers (SPIE) [DOI: [10.1117/1.OE.52.8.081607](https://doi.org/10.1117/1.OE.52.8.081607)]

Subject terms: telescope controller; controller area network; graphical user interface; proportional integral controller; parameter estimation; twin-motor drive; normal loading; LaTeX.

Paper 121589SSP received Oct. 31, 2012; revised manuscript received Mar. 21, 2013; accepted for publication May 2, 2013; published online May 31, 2013.

## 1 Introduction

The 50/80 cm Schmidt telescope at Aryabhata Research Institute of Observational Sciences (ARIES) is an  $f/1$  equatorial system with a usable aperture of 50 cm diameter.<sup>1</sup> Each of its axes is driven by two torque direct current (DC) motors and the motion is sensed by an on-shaft absolute encoder and an incremental encoder coupled through a friction roller. By applying unequal torque on the two motors, backlash-free motion reversal can be achieved. This telescope being relatively small, a simple distributed control architecture based on low cost microcontrollers is being developed. For small systems, an embedded controller reduces the design complexities and offers reasonably good performance. The distributed control system based on microcontrollers has been used in many telescope and mirror control systems.<sup>2-5</sup>

The heart of the hardware system is the axis controller whose objective is to provide accurate tracking and pointing in sky. As tracking performance in a telescope is most critical, in this paper we discuss in detail the velocity control aspects of the axis using a low cost controller based on a dsPIC microcontroller. The final objective of the controller is to track the sky at a constant speed of 15 arc sec/s with an accuracy of 1 arc sec/s ( $4.85 \times 10^{-6}$  rad/s). For modeling the electromechanical telescope system, mechanical parameters were determined experimentally and electrical parameters were used from the motor datasheets. The telescope axis model is approximated using a linear model lumped mass model and a standard tuning chart is used for obtaining

the proportional integral (PI) tuning parameters. The telescope model is simulated in Matlab with a set of suitable tuning parameters and the performance at higher speeds was compared with the actual response of the setup. In practice, the inherent nonlinearities present in the system, like friction, backlash and commuting effects, lead to deviation from the desired behavior and start dominating the response at low speeds. At slow speeds over 2 deg/s, the PI controller performs accurately within an error band of 1%. The effect of nonlinearities become very prominent at fine speeds and limit cycles are introduced due to nonlinear dynamics of friction.<sup>6</sup> These undesired behaviors may be reduced electronically using an additional nonlinear compensator.<sup>7</sup> We preferred first reducing the friction mechanically by reducing the preloads (normal loading) on the drive bearings. This reduced the effect of nonlinearities and resulted in significant improvement in the linear controller tracking performances.

Most of the embedded controllers offer dedicated hardware modules for interfacing different sensors, generating waveform for the actuators and performing serial communication. A set of prototype boards based on 8 and 16 bit PIC microcontrollers comprising the telescope control hardware has been designed. Both RS232 and controller area network (CAN) functionalities for communication have been implemented on each board. Currently, the basic telescope controller using five boards interfaced to PC directly through five RS232 serial ports are enabled for characterizing tracking, pointing and focusing performances. This basic system provides PI control for slew, set, guide, fine and tracking motions, interfaces with the encoders and controls the stepper motor of the focusing system. A remote PC hosting the

graphical user interface (GUI)-based telescope control software is used only for exchanging the user commands otherwise the telescope controller operates stand-alone. This software developed under Microsoft Visual C++ runs multiple threads for hosting GUI, hardware communications and data logging service.

The paper is organized as follows: we present the overview of the telescope structure and mechanism in Sec. 2, and the control electronics and hardware aspects are discussed in Sec. 3. In Sec. 4, we discuss in detail the design, parameter estimation and performance of the PI controller at different velocities, while an overview of the software aspects is given in Sec. 5 and finally concluding remarks are presented in Sec. 6.

## 2 Overview of the 50/80 cm ARIES Schmidt Telescope

### 2.1 Telescope Structure

The telescope as shown in Fig. 1 is located in the Northern hemisphere at a latitude of  $29^{\circ}22'$  and a longitude of  $79^{\circ}27'$  and supported on an off-axis equatorial mount. For smaller telescopes, equatorial mount is preferred as it simplifies the drive and servo controller design. If the polar axis is aligned accurately, the tracking can be achieved by controlling the right ascension (RA) axis alone. The off-axis tube is counter balanced by dead weights and gear box mounted on the other side. Inside the tube, at the prime focus a  $9 \mu\text{m}$  pixel,  $4 \text{K} \times 4 \text{K}$  Kodak IMGX 16801E charge-coupled device (CCD) providing a pixel-scale of 3.6 arc sec/pixel will be used.

### 2.2 Drive Mechanism

The gearbox and hence drive mechanism for both RA and declination are identical. The RA gear (Figs. 1 and 2) box housing is anchored to the south pillar with the help of stiff torque arms.<sup>6</sup> Direct drive motors on the axes without an intermediate gearbox offer backlash-free motion but control at low speeds become difficult due to friction dynamics and commutation problems. Usually for such systems, a hydrostatic bearing

arrangement is preferred to minimize the nonlinear static and coulomb friction. In our case, as the accuracies are reasonable, complexities and cost of hydrostatic bearings are avoided and the telescope is supported on hydrodynamic roller bearings. The axes are driven via a three stage gear train (27:113, 21:123 and 17:250) providing an overall reduction of 360.489:1 between each motor and the output shaft. Motors are directly mounted on the input gear shafts to avoid use of couplings. To avoid backlash in the gears, each axis is driven by a set of two identical motors coupled to the bull gear of polar axis through two identical gear trains. Between the two motors the backlash angle is approximately 42 deg and since the gearbox is symmetrical, the backlash angle between each motor and the main axis bull gear is approximately 21 deg. The two motors provide unequal torque to the bull gear such that if one motor leads the motion in forward direction, the other motor applies a counter torque lagging the motion by the backlash angle, and vice versa for the reverse direction. This technique ensures that teeth contact is never lost between any of the gears during motion reversal and thus a dead zone is avoided. A friction roller assembly is available on the top of the gear box for mounting an incremental encoder. This arrangement allows backlash-free accurate velocity measurements through a reduction of 735:30 (or 1:24.5). For position measurements, an absolute encoder is mounted directly on the extended shaft of the main axis at the center of the gearbox. Provisions have been made for mounting incremental encoders or tachometers directly on the four motors and auxiliary encoders at the bottom of the two gear boxes through a reduction of 1:10.8. Table 1 shows the mechanical specifications of the telescope. These specifications are used for designing the PI controller.

## 3 Electronics and Hardware Design

### 3.1 Telescope Control System

The overall telescope control system is broadly divided into stand-alone telescope control hardware and PC based software for user command. The controller hardware consists

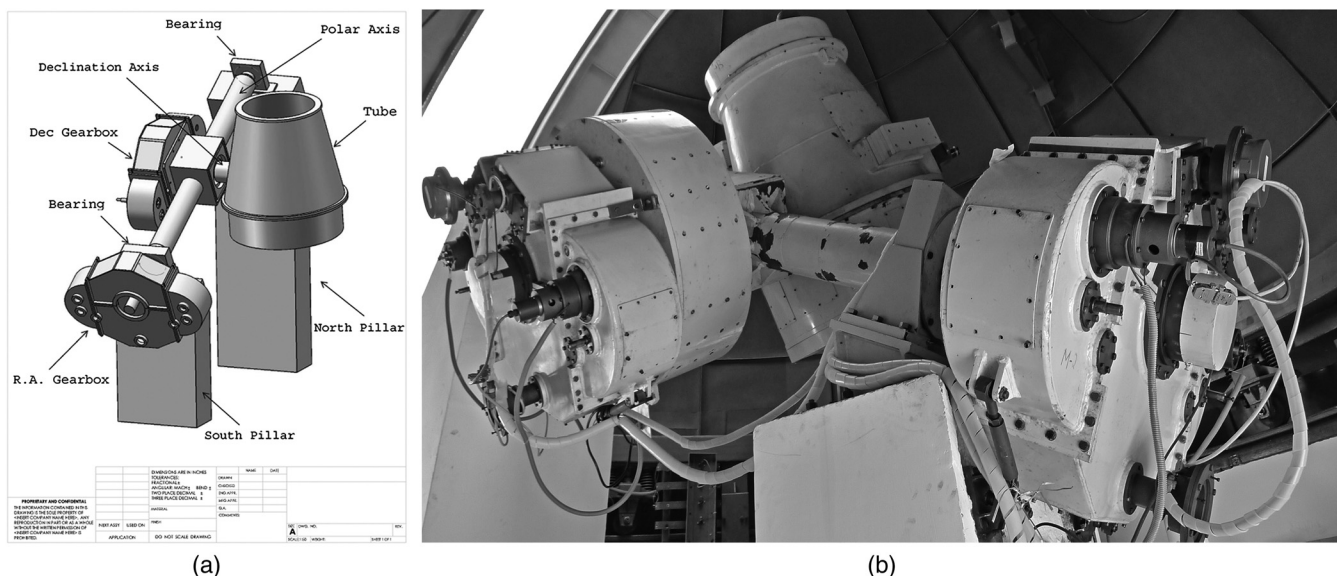


Fig. 1 The 50/80 cm Schmidt telescope: (a) schematic of the telescope, (b) actual telescope installed at ARIES.

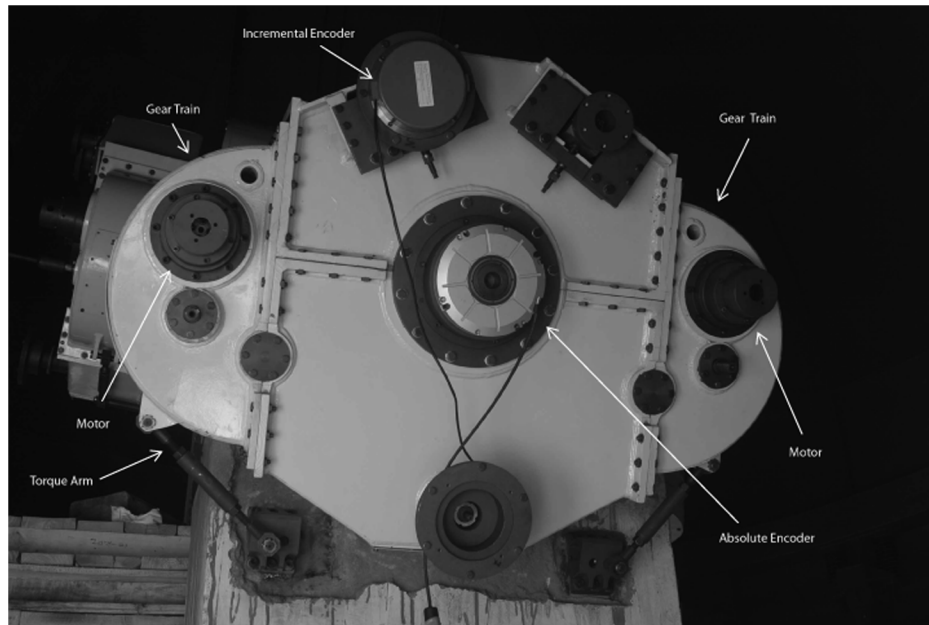


Fig. 2 RA gear box with the control components.

of multiple low-cost PIC microcontrollers performing tasks like interfacing the encoders, providing a linear PI control action to the axes, controlling the focus etc. Currently, for testing the basic functionality, dedicated RS232 ports on the boards are used. The final telescope control architecture would be implemented as a distributed network on the CAN bus. Although the number of controllers appear to be higher, most of the hardware and embedded software design for the boards have been kept common. This facilitated simplicity in design and development whereas efforts were required only for implementing specific functionality.

### 3.2 Control Components

Each axis is driven by two hollow shaft QT-3124 Kollmorgen brushed permanent magnet torque DC motors.

Table 1 Design parameters for the RA and declination drives.

Parameter	Polar axis	Declination axis	Units
Inertia	$2.2 \times 10^6$	$5.79 \times 10^5$	N mm s <sup>2</sup>
Stiffness	$3.08 \times 10^9$	$2.46 \times 10^9$	N mm/rad
Lock rotor frequency	5.96	10.37	Hz
Slewing speed	12.583	12.583	rad/s
Angular acceleration	12.583	12.583	rad/s <sup>2</sup>
Load torque at start	933	316	N mm
Counter torque (25%)	233	79	N mm
Starting torque	1166	395	N mm
Running torque	791	186	N mm

These motors are available in a frameless pancake configuration, i.e., large diameter and a narrow width, and assembled directly on the gear shaft. The motors operate at 24 V DC and are capable of continuously providing stalling current of 6 A. For velocity feedback 4.608 million ppr Gurley series 8 × 60 incremental encoder is used. Through a reduction it provides an overall resolution of 0.011 arc sec accurate upto 0.05 arc sec. A 29 bit RCN829 Heidenhein hollow shaft absolute encoder provides direct measurement of the output shaft position at a high resolution within an accuracy of 0.5 arc sec. Each motor is coupled to a CP-850 incremental encoder which functions as a digital tachometer. Also a 17 bit A25s Gurley absolute encoder with an accuracy of ±15 arc sec is mounted with a 1:10.8 reduction, which acts as an auxiliary encoder for cross checking the position values generated by the on-shaft main encoders.

The focus mechanism slides on a precise THK ball screw arrangement which travels 5 mm/revolution. The mechanism is coupled to a Superior Electric KM062 bipolar stepper motor using a timing belt and pulleys offering a reduction of 1:2. The motor has a incremental shaft encoder for position measurement and a PCA-116 series linear variable differential transformer (LVDT) is used for referencing. The motor and on-shaft encoder undergoes four full rotations generating four index pulses in the range ±5 mm. At 0.9 deg per half step the housing can be positioned with a resolution of 6.25 μm.

### 3.3 Schematic of the Controller

The main components of the controller hardware include pulse width modulation (PWM) based PI controllers for the twin-motor drives, interfacing electronics for the encoders, bipolar stepper motor controller for focusing, power amplifiers for the motors, and a communication system. Owing to similar mechanical drive systems, the controller hardware design remains the same for both RA and declination axes. Currently, pointing is implemented with the help of slew, set, guide, fine motions requiring user

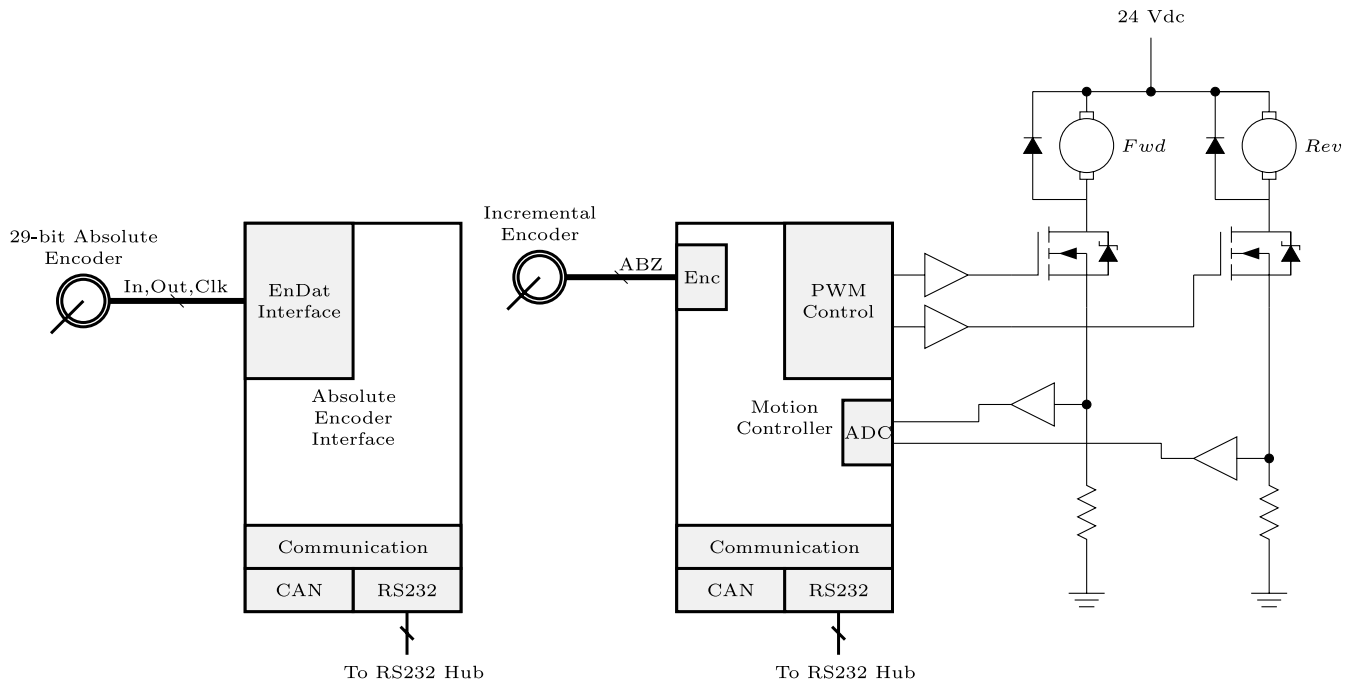


Fig. 3 The schematic of the axis controller.

intervention. These set of velocities for both axes and tracking velocity for RA are maintained constant with the help of the PI controller. The schematic of the axis controller and focus controller are shown in Figs. 3 and 4 respectively. Each motion controller is implemented on a separate dsPIC30f3011 microcontroller running an incremental PI control algorithm in PWM mode.<sup>6</sup> It provides the control signal for both the motors on two of its PWM output channels. For driving the two motors, two IRF250 power MOSFETs along with the driver stage are used to amplify the PWM signals. For reducing the mechanical backlash, the PWM duty cycles on the two channels are adjusted such that 100% of the control effort is applied on the forward direction motor and 10% to 25% on the reverse direction motor. In case of the linear controller, the effect of applying opposite torque using second motor is accounted simply using superposition. Each motor is connected between 24 V DC supply

and the drain terminal of MOSFET with a 0.1 ohm resistance between the source terminal of MOSFET and ground. The voltage across the resistance is filtered and captured using analog to digital converter (ADC) channels of the dsPIC for determining the motor armature current. The ADC module is synchronized with the PWM module using an interrupt to capture the samples during the PWM falling edge where the motor current peaks. The encoder feedback module of dsPIC is used for capturing encoder pulses from the incremental encoder for estimating the velocity. The interrupt routine is used to ensure a fixed sampling time of 5 ms.

Another set of boards are developed using PIC18f4480 microcontroller to interface the on-shaft Heidenhein position encoders on synchronous serial ports. The encoder provides serial data packets on the bidirectional EnDat2.2 interface, which is decoded by the microcontroller for determining the absolute shaft position. The position measurements are

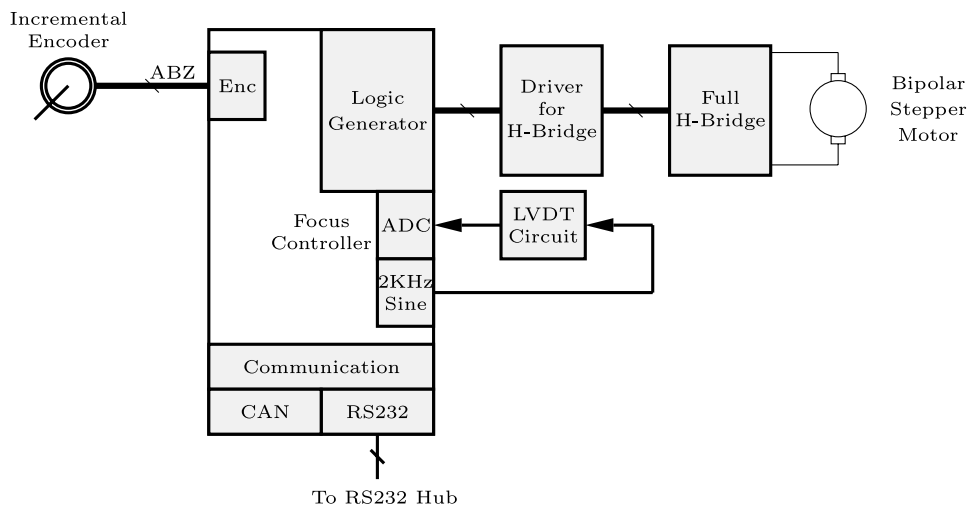


Fig. 4 The schematic of the focus controller.

displayed on GUI and used for setting soft limits on the telescope extremes.

For controlling the focusing mechanism, a single microcontroller board was developed around PIC18F4431. Its encoder feedback module is used for interfacing the

incremental encoder on the motor shaft. The controller also generates a square wave at a 2 KHz frequency on its PWM channel. This is filtered using an active bandpass filter and amplified to obtain a fundamental 2 KHz sine wave for the primary coil of the LVDT. The output of the LVDT is

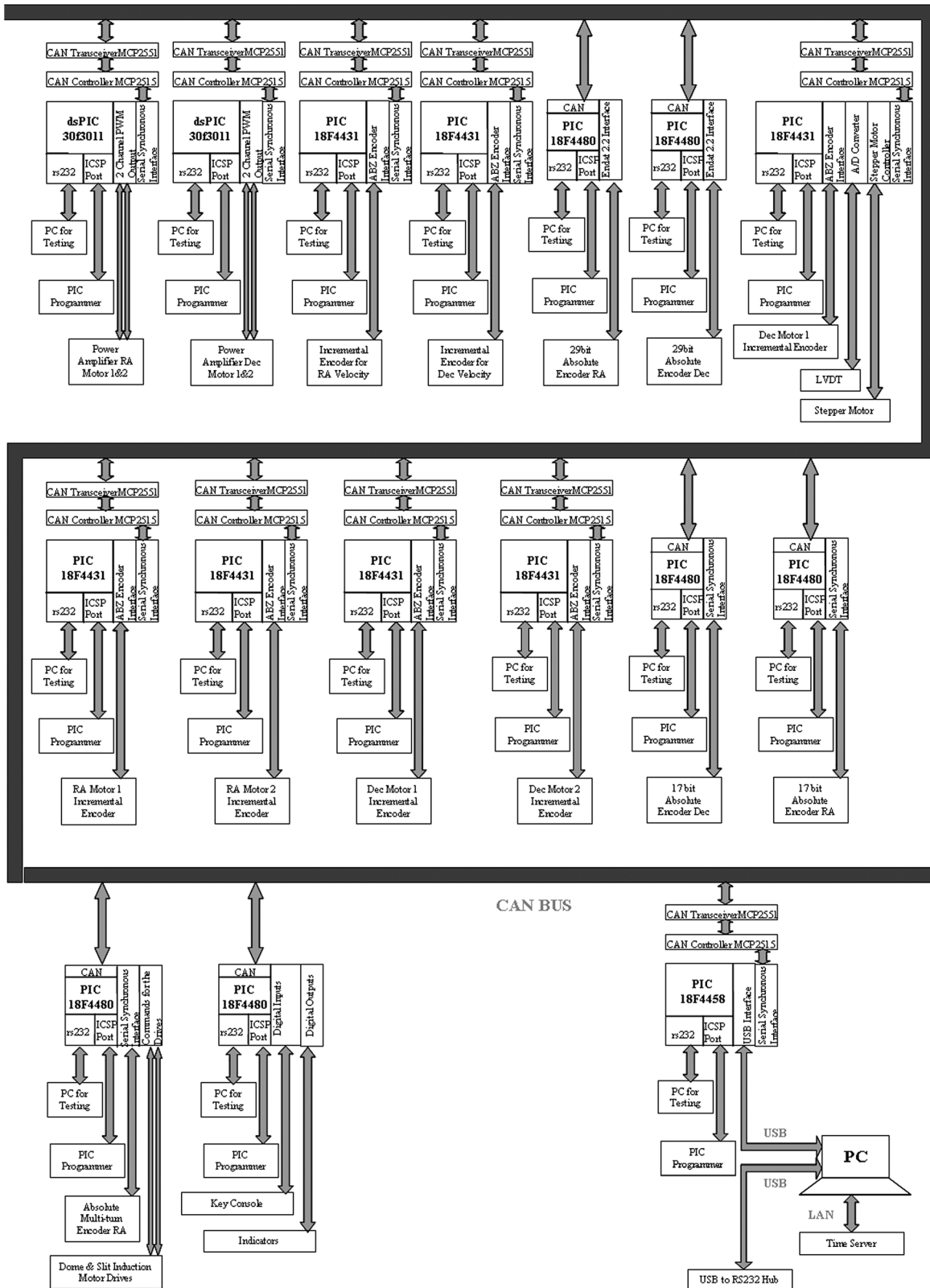


Fig. 5 The schematic of the overall system under development.

sampled by a 10 bit ADC channel of the controller and combined with the index pulse of the encoder for absolute referencing. The bipolar motor is driven by a dual H-bridge in half stepping mode and consumes 1.2 A per coil at 4 V DC during operation. To prevent generation of heat during holding, the motor is kept in regenerative mode through the free-wheeling diodes.

### 3.4 Message Timing and Communication

All boards consist of peripherals for CAN interfacing, asynchronous serial communication (RS232) and serial debugging and programming. For the board with PIC18F4480, the inbuilt CAN controller is used whereas for rest of the controller boards, a MCP2515 CAN controller is used. The final distributed telescope controller would have over sixteen microcontroller boards on the CAN bus as shown in Fig. 5. A CAN-to-USB board has been developed on a PIC18F4550 for putting the commanding PC on CAN bus. The communication bandwidth requirement between the commanding PC and hardware is very low, therefore the USB device is configured as a simple plug and play human interface device (HID).

CAN is a standardized reliable system from real-time communication and has been successfully used in many telescope systems and subsystems.<sup>8-12</sup> A CAN bus supports upto 1 Mbit/s for a total bus length within 40 m. The distributed boards allow modularity, scalability, use of low cost micro-controllers, easy debugging, and possibility of locating the boards closer to the sensors. Modularity and scalability allows independent development as well as the addition of other boards as nodes to the existing network. Currently, 10 nodes providing position and velocity measurements

for the two axes, velocity measurements for the four DC motors, digital display unit, along with USB-to-CAN node were tested in lab. The data word size per board is 8 bytes, first byte representing the device type. A total of 64 bytes are exchanged between the USB-to-CAN controller and the interfacing PC. The CAN network is yet to be implemented on the telescope.

For the purpose of telescope testing and characterization, only the PI controller boards, position measurement boards and focus controller board implementing the basic functionalities are utilized. These boards are independently connected to an 8 port RS232 hub for PC interfacing. Time stamped data packets each containing 25 sets of 10 ms samples of PI control effort, telescope position, telescope velocity, ADC counts and focus position are continuously transferred to the interfacing PC at a fixed interval of 250 ms on five RS232 serial ports. The data is displayed on the GUI and continuously logged in the PC.

## 4 PI Controller Design and Performance

For reducing errors at different speeds and achieving control at fine speeds, it is necessary to develop a suitable feedback controller. For example in Fig. 6, we compare the system velocity responses at higher speeds in both an open loop condition and a closed loop control condition at reduced bearing preload. Without a feedback controller, the peak error reaches up to 15% and also limit cycles are more prominent whereas the feedback control improves the performance and limits the peak error close to 7%. As the oscillations are both due to imbalances and friction and in the open loop without using a controller, it is not possible to reach speeds below 100 arc sec/s due to excessive friction. In Fig. 7, we

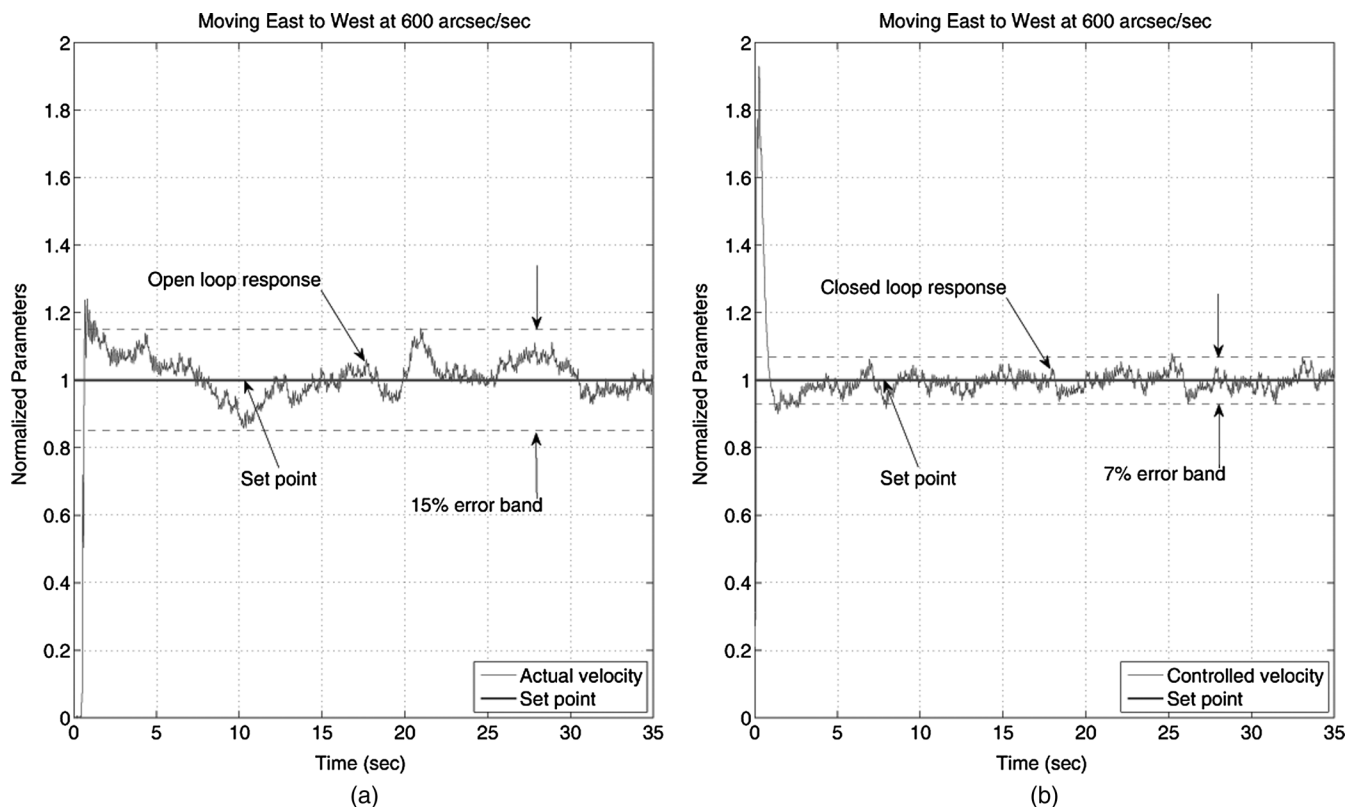


Fig. 6 (a) Open loop response at high speed, (b) closed loop response at high speed.

compare the system velocity responses at 100 arc sec/s in both open loop conditions and closed loop control conditions at reduced bearing preload. Here again in absence of a feedback control, the errors are quite high and some low frequency oscillations close to 0.05 Hz are riding on the velocity response whereas the feedback control filters out the low frequency errors and also reduces the error band. Although lower speeds can be achieved using a controller, the control system characteristics changes at such speeds as the effect of friction dynamics and disturbances due to imbalances in the gears become more pronounced.

The 50/80 cm ARIES Schmidt telescope is required to continuously track the sky at a very low speed of 15 arc sec/s maintaining an accuracy of 1 arc sec/s. At such low speeds, the dynamics of friction starts dominating the overall response of the system. The response becomes highly nonlinear, making it difficult to control using a linear controller. The nonlinear model of the telescope is given by the following set of equations:

$$v = L \dot{i} + Ri + K_{\text{motor}}\omega \tag{1}$$

$$K_{\text{motor}}i = J_r \ddot{\omega} + T_{\text{friction}_r} \tag{2}$$

$$T_{\text{friction}} = \sigma_0 \dot{\theta}_z + \sigma_1 \ddot{\theta}_z + \sigma_2 \omega \tag{3}$$

$$\ddot{\theta}_z = \omega - \frac{|\omega|}{g(\omega)} \theta_z \tag{4}$$

$$\sigma_0 \cdot g(\omega) = T_C + (T_S - T_C)e^{-(|\omega|/\omega_s)^\delta}, \tag{5}$$

where  $v$  is the applied voltage,  $i$  is the armature current  $R$  and  $L$  are the armature resistance and inductance respectively,  $K_{\text{motor}}$  is the motor constant,  $\omega$  represents the angular velocity of the motor and  $\theta_z$  represents the micro-displacement.  $J_r$  is the reflected moment of inertia at the motor shaft and  $T_{\text{friction}_r}$  is the reflected friction at the motor shaft.  $\sigma_0, \sigma_1, \sigma_2, T_S, T_C, \omega_s$  are the six parameters of the LuGre model for friction<sup>13</sup> and  $\delta$  is the empirical parameter. The function  $g(v)$  captures the Stribeck effect.<sup>14</sup> By reducing the preload on the bearings, the effect of friction can be reduced to an extent such that a linear controller starts providing a reasonable performance. A discrete time PWM-based PI controller is designed for the lumped mass model based on the electromechanical parameters of the telescope. The transfer function of linear time invariant second order model describing the telescope axis model reflected at the motor shaft is given by:

$$\frac{\omega}{V - \frac{T_{S_r}R}{K_{\text{motor}}}} = \frac{\frac{K_{\text{motor}}}{J_r L}}{s^2 + \left(\frac{R}{L} + \frac{\sigma_{2_r}}{J_r}\right)s + \left(\frac{R \sigma_{2_r}}{L J_r} + \frac{K_{\text{motor}}^2}{J_r L}\right)}, \tag{6}$$

where  $J_r, \sigma_{2_r}$  and  $T_{S_r}$  are the inertia, linear viscous friction, and stiction respectively reflected at the motor shaft. In Eq. 6 only, the stiction and the viscous friction components of friction are considered and the term  $T_s L/K$  is neglected as the inductance is very small. Discretization at a sampling rate of  $\Delta t$  introduces a dead time of  $\Delta t/2$ . The overall system can be represented using a second order system plus dead time model and standard tuning rules of PI control can be applied.<sup>15</sup>

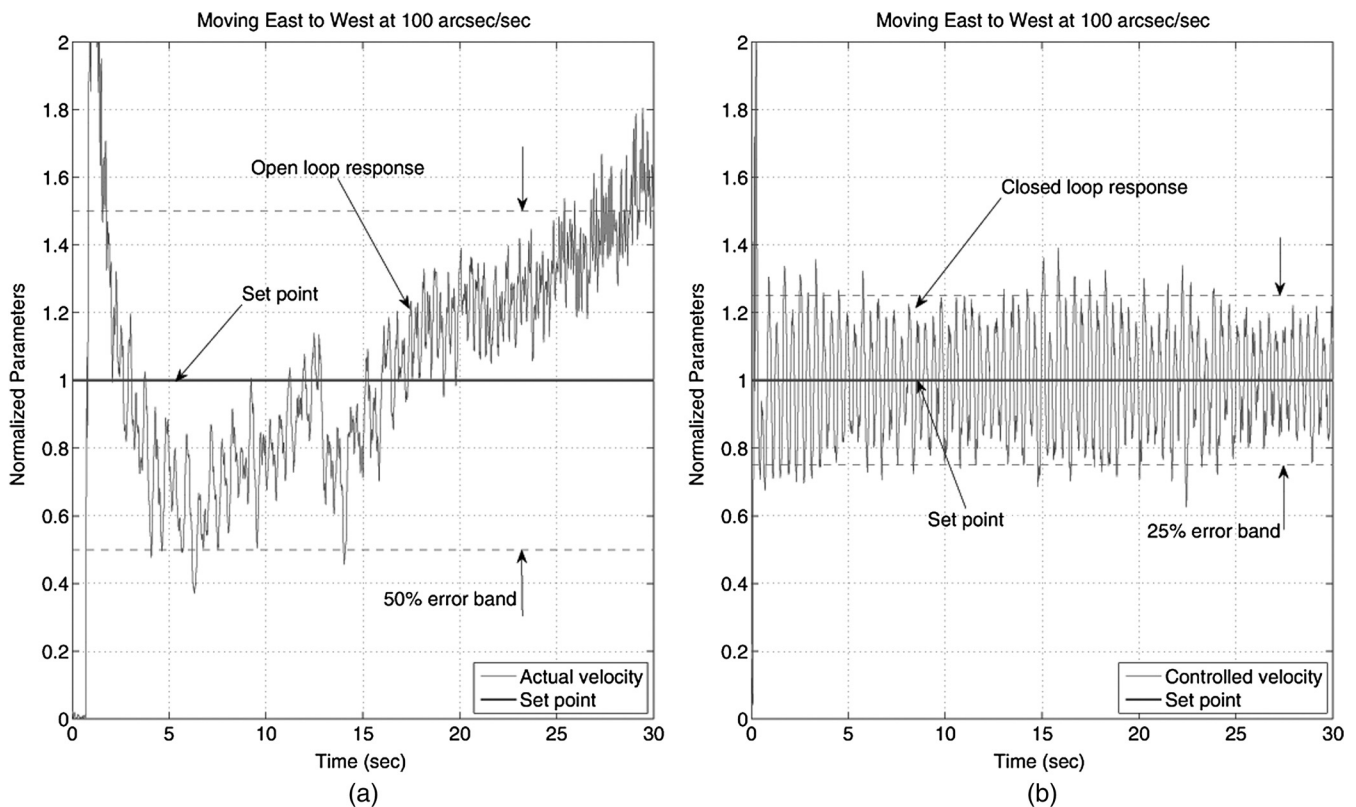


Fig. 7 (a) Open loop response at low speed, (b) closed loop response at low speed.



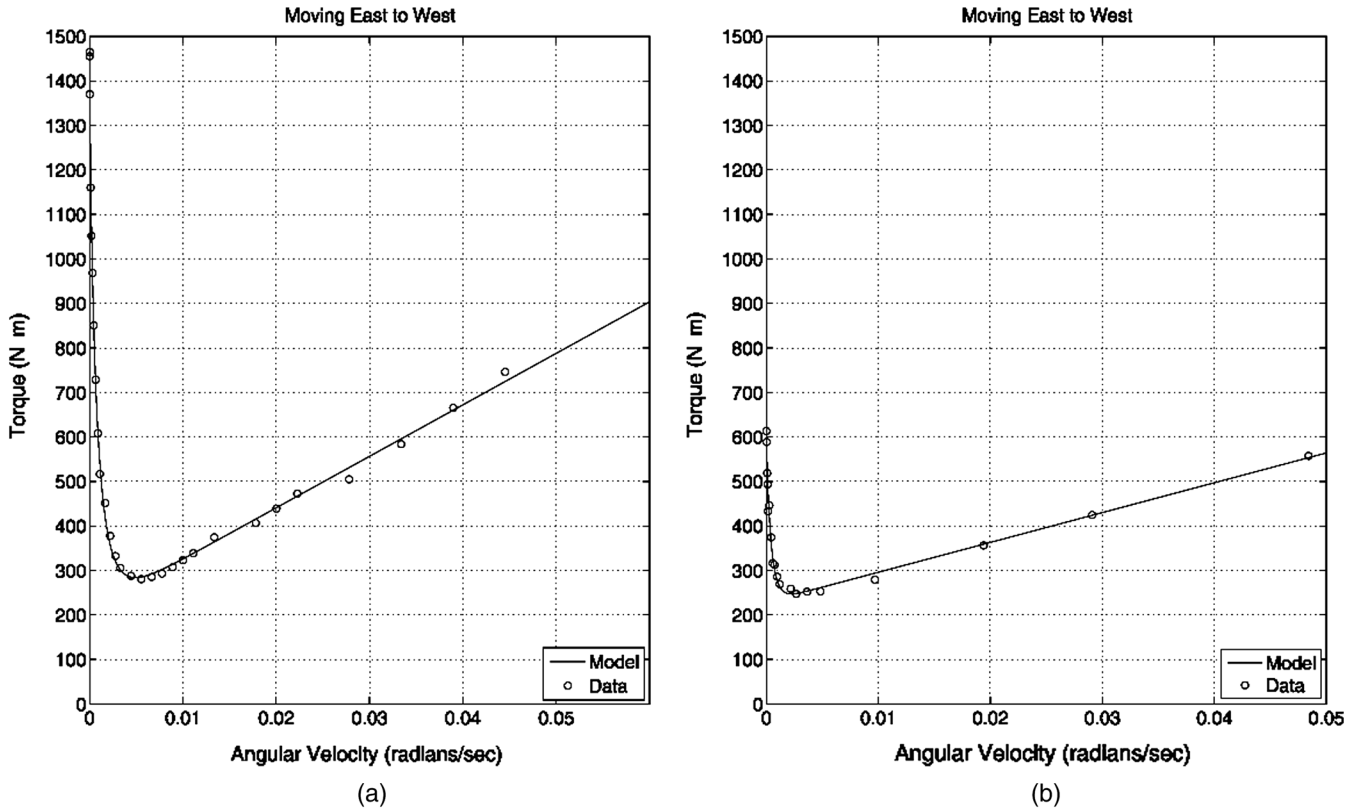


Fig. 8 (a) Friction characteristics at high bearing preloads, (b) friction characteristics at reduced bearing preloads.

In the controller hardware design, the incremental linear PI control algorithm<sup>16</sup> of the following form is implemented using dsPIC30f3011 microcontroller, which ensures a bumpless transfer between different speeds during pointing operation.

$$\begin{aligned}
 E_k &= (\omega_{sp} - \omega_k) && \text{Error} = \text{setpoint-output} \\
 dU_k &= K_p(E_k - E_{k-1}) + K_i(E_k) && \text{Incremental PI control} \\
 U_k &= U_k + dU_k && \text{Control effort to plant}
 \end{aligned}$$

Here  $E$  is the error representing difference between the desired velocity  $\omega_{sp}$  and the actual velocity  $\omega_k$ ,  $U_k$  represents control command at  $k$ th instant,  $\delta U$  represents incremental control command,  $K_p$  and  $K_i$  represent the  $P$  and  $I$  gains respectively. The duty cycle of the pulse width modulator is modulated using the control effort  $U_k$ . To prevent integral wind-up, upper and lower limits are imposed on the  $U_k$  before loading the PWM duty cycle register. During the design, torsional effects and all inertias that are small compared to the load are neglected.

To perform simulations and for tuning the controller, telescope parameters were experimentally determined using various test inputs. During telescope installation, the normal loading on the bearings were high, resulting in excessive friction. The normal loading on the bearings was reduced and also some of the dead weight was removed around the declination axis of the system for reducing the moment of inertia. The telescope friction parameters are determined at both actual and reduced preload conditions by fitting the LuGre friction characteristics in the torque velocity map as shown in Fig. 8. This map is obtained by running the telescope at

different steady state velocities and measuring the corresponding motor armature current.<sup>6</sup> The following parameters (Table 2) of the telescope were obtained from the friction characteristics.

As the inertia of the system was reduced, it was estimated by performing a rundown test.<sup>17</sup> In a rundown test after reaching a steady state speed, the input torque is set to zero for obtaining the deceleration characteristics as shown in Fig. 9. As the applied voltage and electrical model of the motor are known, copper losses in the armature can be calculated. From the deceleration curve and friction characteristics, the moment of inertia was determined<sup>17</sup> to be  $J = 1.76 \times 10^6$  N-mm sec<sup>2</sup>. Using the estimated parameters, the telescope model with PI control was first simulated on Matlab simulink as shown in Fig. 10 and the simulink response for higher velocity of 600 arc sec/s is shown in Fig. 11. Since the friction is mostly linear at these speeds and the approximated linear model is valid, the response of the actual telescope and simulated model are similar. For

Table 2 Estimated parameters of the telescope about the RA axis.

Parameter	Low preload	High preload	Units
$\sigma_2$	$67 \times 10^2$	$113 \times 10^2$	N m s/rad
$T_c$	229	217	N m
$T_s$	621	1490	N m
$v_s$	$4 \times 10^{-4}$	$7 \times 10^{-4}$	rad/s

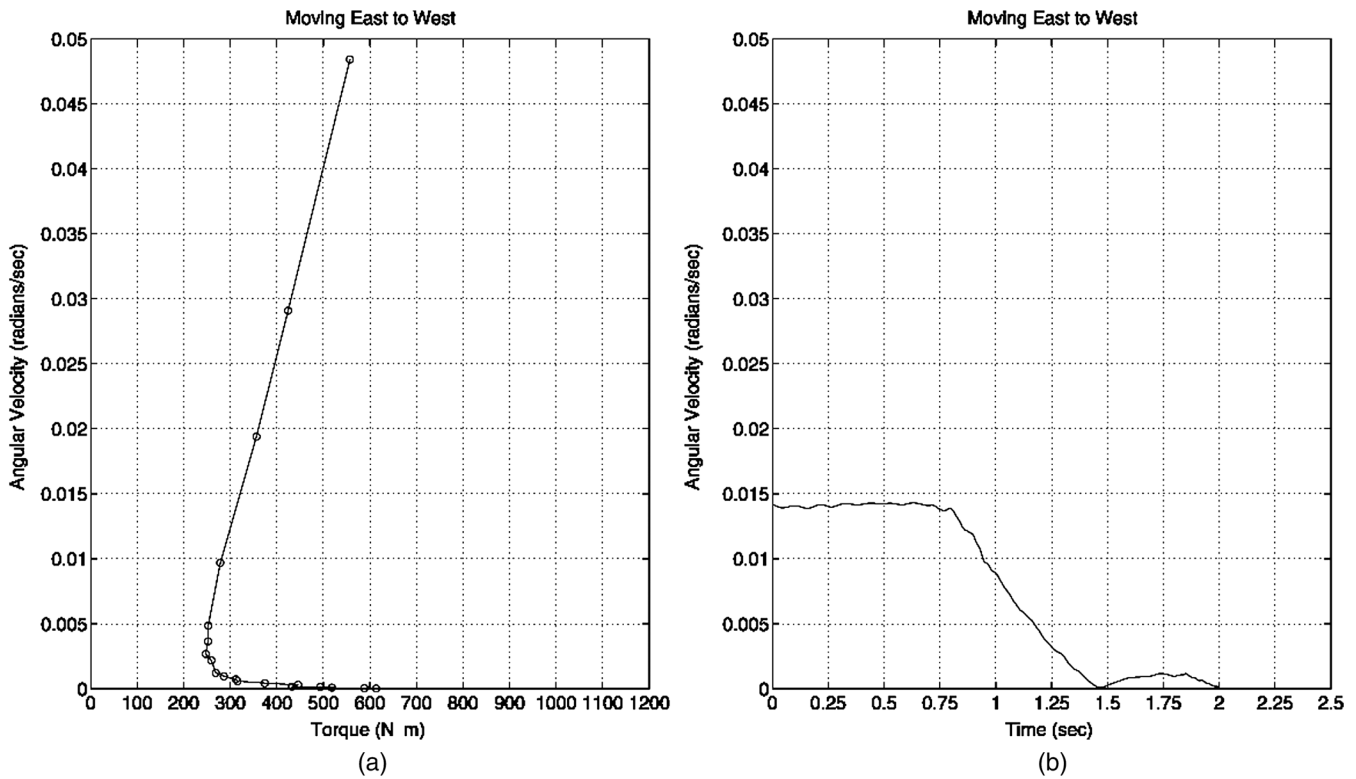


Fig. 9 Characteristics of the rundown test. (a) Steady state velocity versus friction torque map, (b) velocity versus time deceleration characteristics.

lower velocities, our simulation results showed oscillations due to stiction which may be reduced by reducing the PI gains. But at low gains, the actual system exhibits stick slip motion hence we preferred keeping the gains high. Since the errors are low at higher speeds where the telescope operates in linear regime of friction, it may be possible to improve the low speed performances by reducing friction-induced nonlinearities.

The response of the actual system with a controller keeping current loop open and velocity loop closed for different velocities are shown in Figs. 6, 12, and 13. Near the tracking speeds, the limit cycles exhibited by nonlinear friction dynamics become more prominent and results in a jittery motion. During excessive preload, the peak errors introduced by the jitters at tracking speeds under PI control are very high. The performance improved when the bearing preload was carefully reduced avoiding excessive axial ply which is shown in Fig. 13 and the peak error comes down to 25%. At

higher speeds of 600 to 1000 arc sec/s, the peak errors are within the 2% to 7% range as the the telescope operates in the linear viscous friction regime. The error band improves at even higher speeds and we found that the peak errors are within 1% at slow speeds in the range of 1 to 3 deg/s.<sup>18</sup>

## 5 Software Design

### 5.1 Overview of the Software

The telescope control software was developed in Visual C++, which basically provides a GUI and communicates with the control hardware. It is capable of communicating with each board directly using multiple serial COM ports as well as with the USB-to-CAN board on USB port. The commands sent to and controller data continuously received from the telescope are logged at a desired interval in ASCII format. Since multitasking software especially performing hardware communications is prone to breakdown, each function is

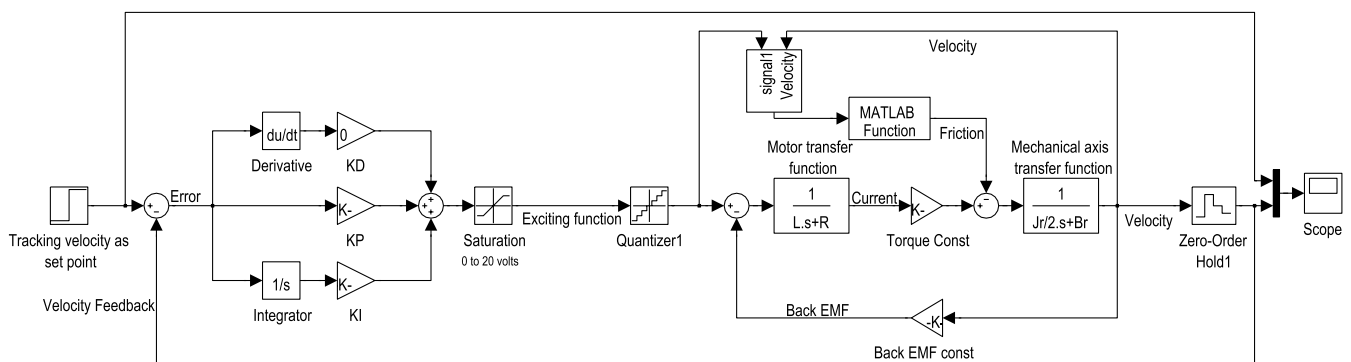


Fig. 10 Simulink block diagram for the linear telescope model.

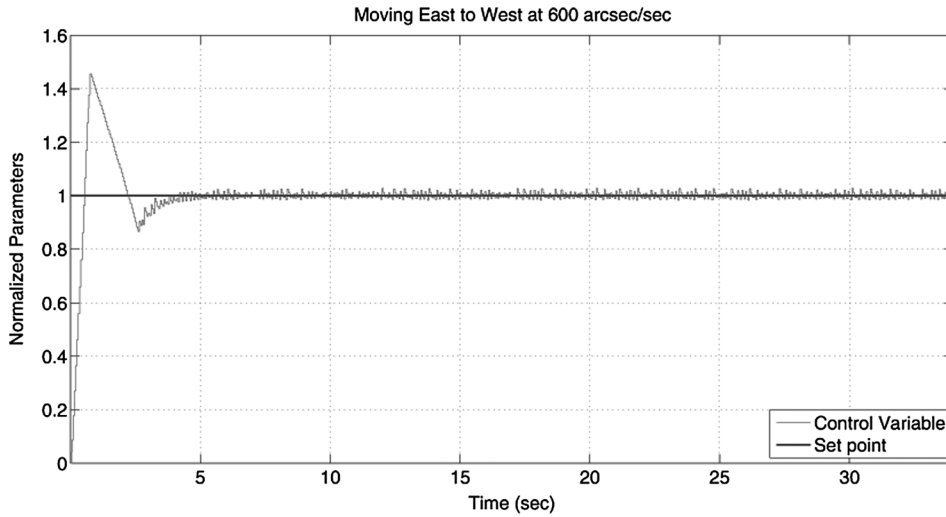


Fig. 11 Response of the Matlab simulation for tracking velocity set point.

implemented separately in a multiple software thread. This provides robustness against communication hardware errors or buffer overflows. When the GUI is launched, more than ten software threads handling communication over several serial ports, a USB port, logging service and GUI are launched and remain active. Multithreading also provides modularity and scalability falling in line with the advantages of the distributed telescope hardware architecture. The GUI offers several floating dialog windows which can be dragged to an extended PC monitor. For device-to-device communication, a CAN interface is provided and preliminary tests

were conducted by sending and receiving 8 bytes per board upto a transfer rate of 1 MHz. The PC picks up CAN messages using USB-to-CAN board configured as a HID device.

### 5.2 Software Aspects

When the software is launched, the main console (Fig. 14) is selected for powering up, manual pointing at preset speeds, tracking and monitoring the telescope parameters. During the power on process, communication with the hardware is performed for a health check. The status window displays

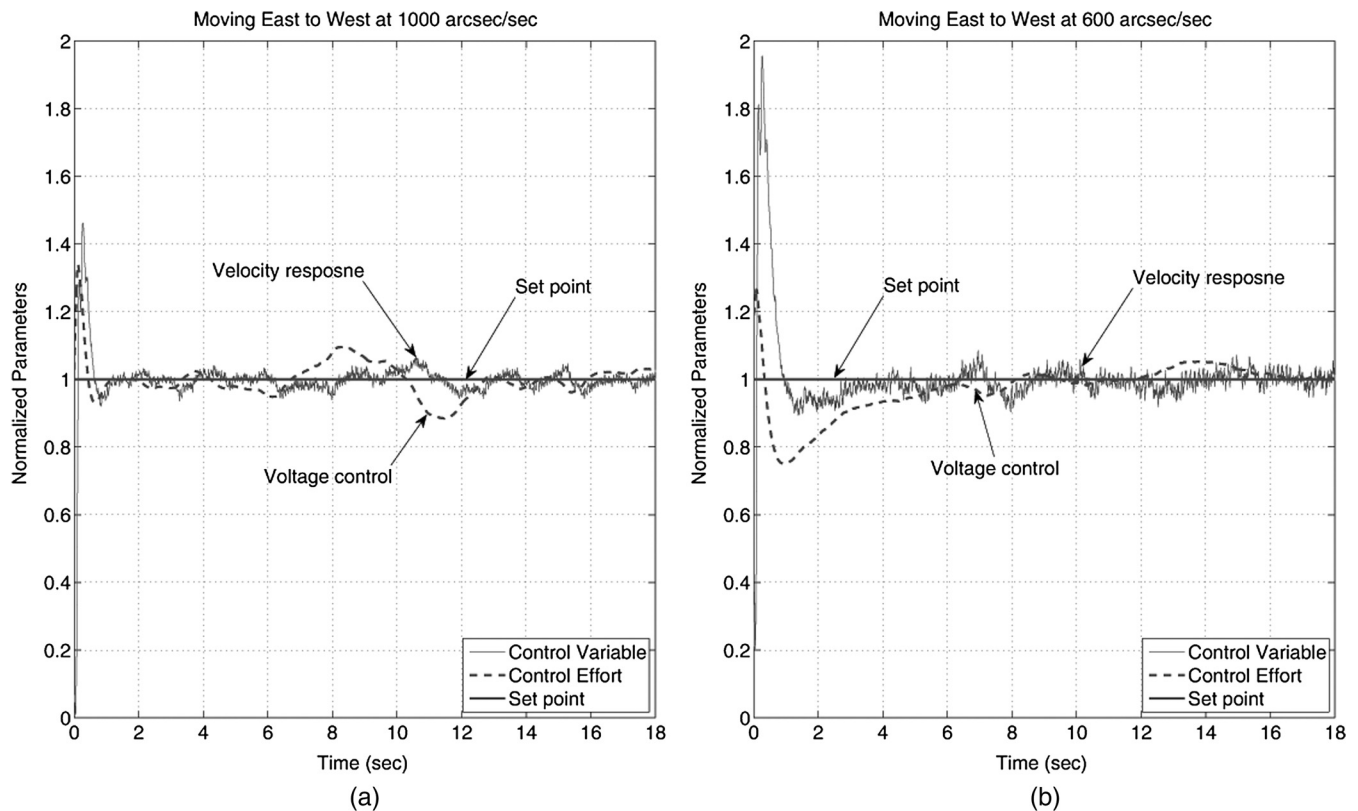
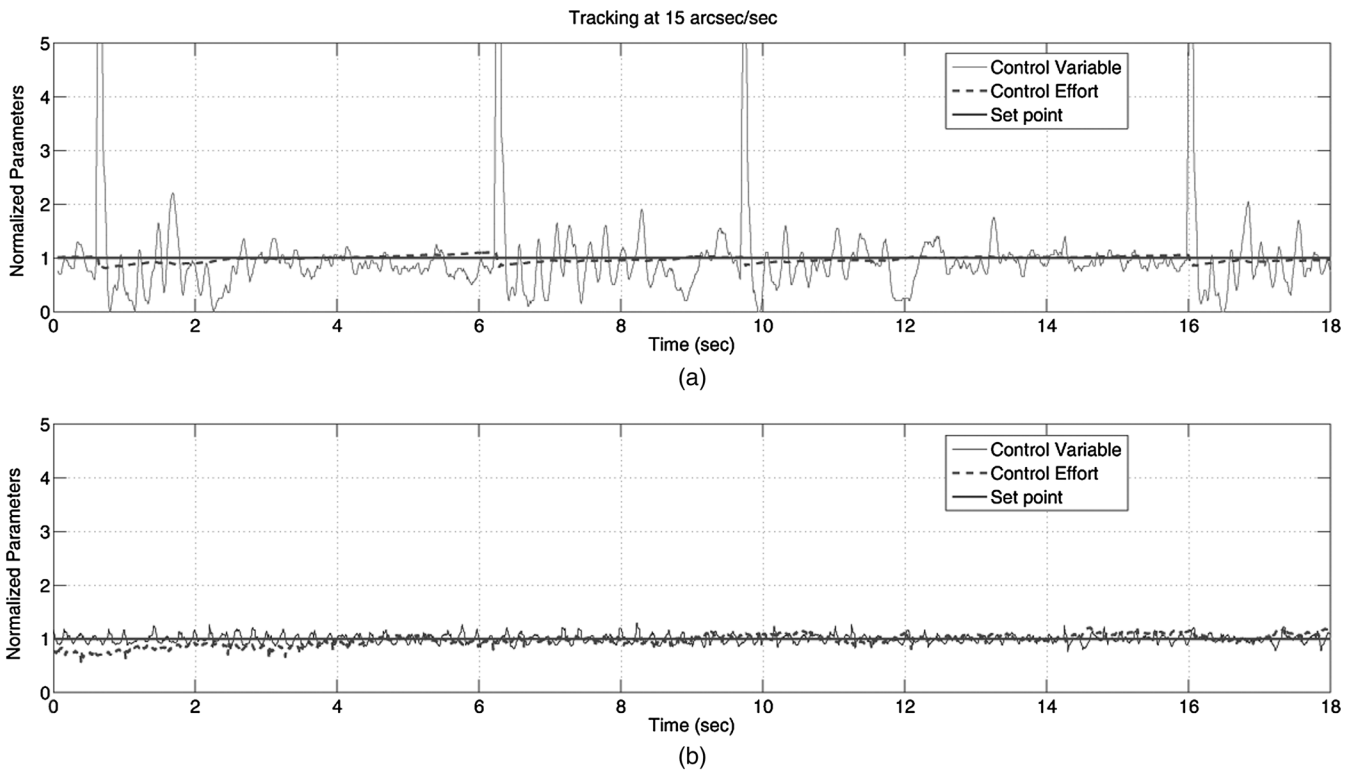
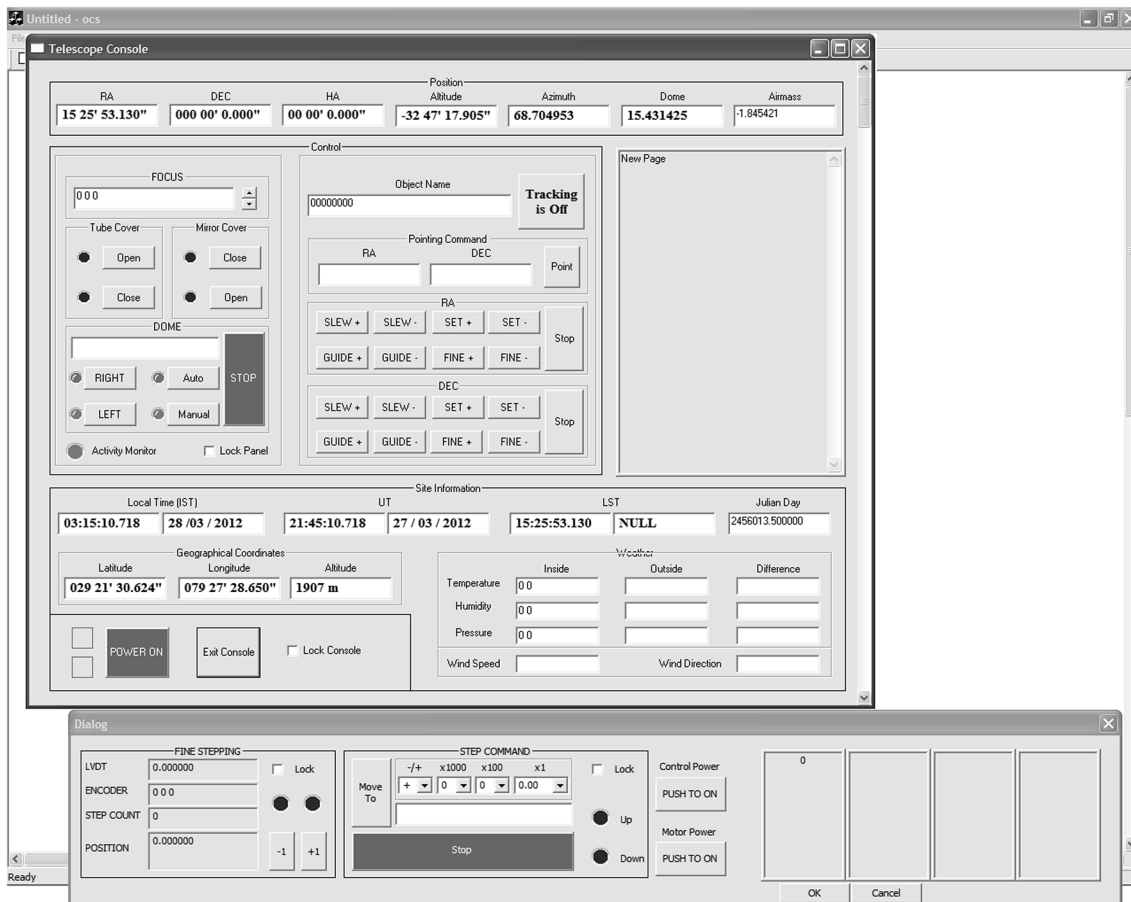


Fig. 12 The controller response at high speeds with reduced preload. The dashed line is the control effort and horizontal line is the desired speed.



**Fig. 13** (a) The controller response at tracking speed with high bearing preloads, (b) the controller response at tracking speed with reduced bearing preloads. The dashed line is the control effort and horizontal line is the desired speed.



**Fig. 14** The consoles for telescope operation.

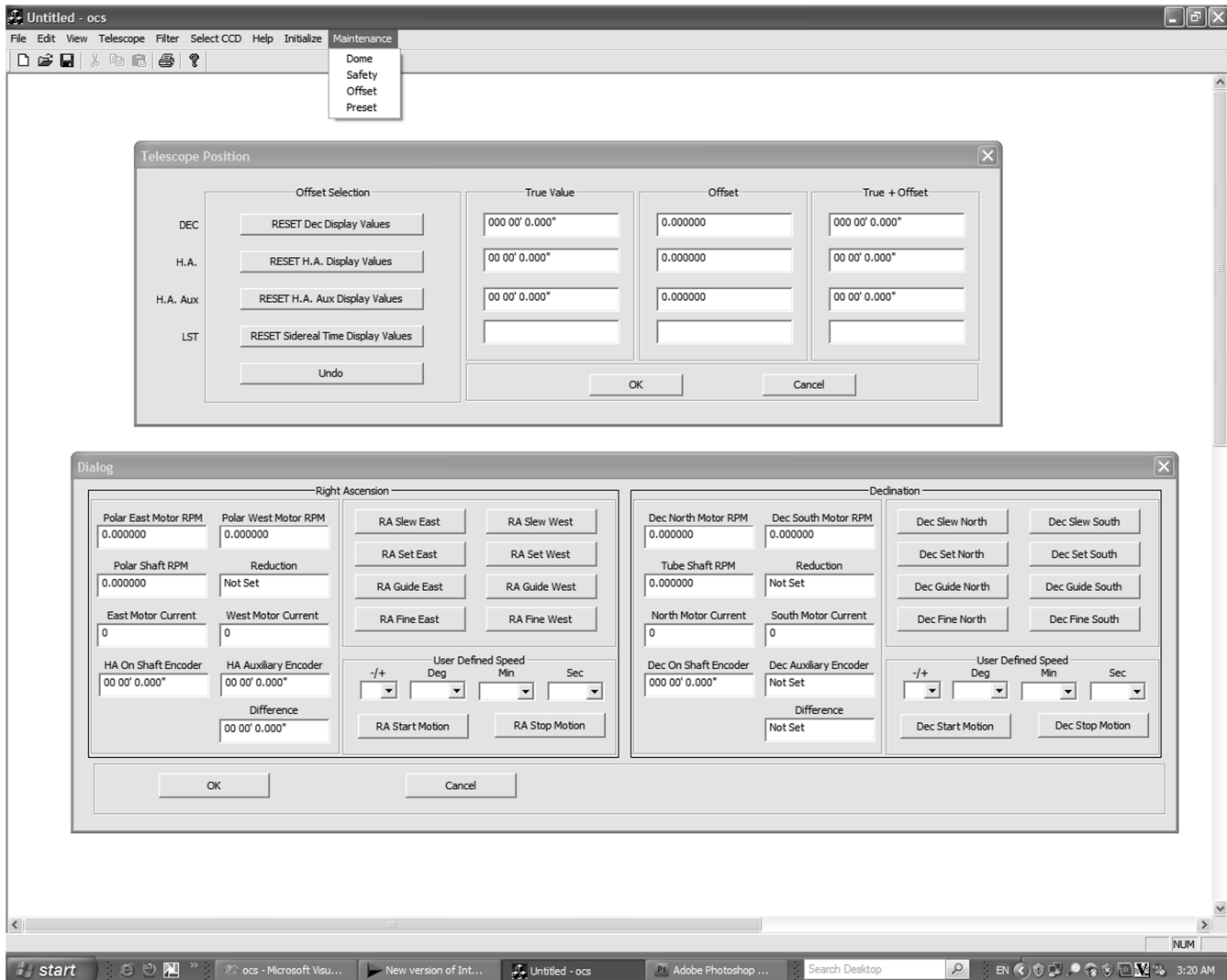


Fig. 15 The consoles for maintenance purpose.

messages related to the user command sequences, messages exchanged with the hardware, system response and errors. The console can be locked, which greys out the buttons to prevent any accidental issue of command. Currently dome and weather stationing control hardware have not been implemented but the features have been implemented and tested in the lab on RS232 ports.

A separate console is launched for operating the focus housing (Fig. 14). The stepper motor can either be moved in single steps by using  $\pm 1$  buttons or moved to a desired position directly by selecting the set position and clicking on Move To button. Virtual LEDs provided on the console start blinking when the motor is running. The motor power OFF button provides holding operation by putting the stepper motor on regenerative mode and Control Power OFF completely frees the motor. The LVDT and encoder values are displayed in the text windows and refreshed every 250 ms.

For monitoring other parameters of the telescope useful for maintenance and troubleshooting, two maintenance consoles have been provided (Fig. 15). The first console is used for alignment of the absolute encoders, i.e., when the telescope position is determined using a reference star,

offsets can be applied on the encoders to match the known telescope position. In the second console, the individual motor currents and the tachometer signals can be monitored. The tachometer readings and the telescope velocity measurements are used for displaying the gear reduction in runtime and logged for analysing the backlash in the gear boxes. Also the auxiliary position encoder readings and its difference from the on-shaft encoder readings are displayed. The auxiliary encoder is used for the purpose of cross checking. This can also be statistically combined with the true encoder readings for generating a better position estimate.

The user command sequence, device status, sensor data and errors are continuously displayed in text windows and simultaneously logged in four separate ASCII files by the data logging software thread. It continuously displays the speed, position and current data and stores it on the hard disk in ASCII format. The rate of log generation can be set as per the need, which is usually kept high during maintenance procedures. One of the key advantages of developing software in-house is the available flexibility for immediate modification, bug fixing and continuous improvement.

## 6 Conclusion

As the Schmidt telescope is a small system requiring a reasonable performance, a telescope controller comprising a set of simple low-cost controller boards was developed. For such a telescope, we favored in-house component-level design of hardware and software to enable effectiveness in maintenance and upgradation activities. Modularity and scalability is maintained in both hardware and software using separate board and communicating thread respectively for each specific task. The CAN functionality is implemented on the boards and tested in the lab; it will be implemented on the telescope at a later stage. For modeling and simulation, the telescope parameters are estimated experimentally and the axes are controlled using a linear PI controller. At higher speeds, the telescope operates in a linear viscous friction regime of friction and hence exhibits much lower levels of error. Both open loop and closed loop performances are comparable at these speeds. There are some control issues at low speeds due to friction dynamics and the open loop performance degrades at low speeds and closed loop control becomes necessary below 100 arc sec/s. These performances were at a reduced preload and the open loop response shows clearly the effect of nonlinear friction. It was observed that the effect of friction lessened on reducing the bearing preload on closed loop performances at low speeds. As a result, the linear PI controller with the system approximated to a SOPD model provided a reasonably good performance at low speeds like tracking speeds keeping the peak errors within 25%. As the telescope equipped with CCD detector provides a pixel-scale close to 3.6 arc sec/pixel, it means the object is sampled in 7.2 arcsec<sup>2</sup>. Considering the wide observing field of the telescope and its large sampling region, a 25% error rate in tracking without an autoguider may be acceptable. The optical performance of the system is yet to be determined, which would help in evaluating the overall performance. The telescope is in a testing phase with the prototype boards and efforts are underway for developing a nonlinear friction compensator to further improve the accuracies. In our previous work we have already characterized the friction present in the system; with the help of the additional encoders installed on the telescope, we would also like to characterize backlash in the gear system and explore nonlinear compensation techniques.

## References

1. K. G. Gupta et al., "Development of 50 cm B-N Schmidt telescope at ARIES," in *Proc. of the 25th Meeting of ASI, 2007*, Vol. 25, pp. 80, Bulletin of the Astronomical Society of India Proceedings, India (2008).
2. J. R. Varsik and G. Yang, "Design of a telescope pointing and tracking subsystem for the Big Bear solar observatory new solar telescope," *Proc. SPIE* **6274**, 62741T (2006).
3. P. Hirsch, K. Reif, and P. Müller, "A new control system for the 1m Cassegrain telescope at the Hoher List observatory," in *Astronomische Gesellschaft Meeting Abstracts*, R. E. Schielicke, Ed., Vol. 15, pp. 113, Astronomische Gesellschaft, Germany (1999).
4. C. Ramiller et al., "A new control system hardware architecture for the Hobby-Eberly telescope prime focus instrument package," *Proc. SPIE* **7740**, 77403H (2010).
5. G. B. Russiniello, D. Huguenin, and F. P. Wildi, "Robust control system for the new 1.2-m telescopes of the Geneva observatory," *Proc. SPIE* **4009**, 216-226 (2000).
6. T. S. Kumar and R. N. Banavar, "Identification of friction in the 50/80 cm ARIES Schmidt telescope using the LuGre model," in

- Proc. of the 18th IFAC World Congress*, S. Bittanti, Ed., Vol. 18, pp. 980-985, Elsevier Limited (2011).
7. C. Rivetta and S. Hansen, "Friction model of the 2.5m SDSS telescope," *Proc. SPIE* **3351**, 466-477 (1998).
8. J. Cortina et al., "The control system of the MAGIC telescope," in *The Universe Viewed in Gamma-Rays*, R. Enomoto, M. Mori, and S. Yanagita, Eds., *International Science Symposium on The Universe Viewed in Gamma-Rays, 2002*, Universal Academy Press, Inc., New York (2003).
9. A. Farris, R. Marson, and J. Kern, "The ALMA telescope control system," in *Proc. of 10th Int. Conf. Accelerator Large Expt. Physics Contr. Syst.*, Joint Accelerator Conferences Website, CERN, Geneva (2005).
10. C. Molfese, P. Schipani, and L. Marty, "VST telescope primary mirror active optics actuators firmware implementation," *Proc. SPIE* **7019**, 701926 (2008).
11. C. Molfese et al., "Survey telescope control electronics," in *Proc. of International Symposium on Power Electronics, Electrical Drives, Automation and Motion*, pp. 523-527, IEEE (2008).
12. B. Lefort and M. P. Puig, "GTC a CAN based controlled telescope," in *Proc. of the 12th International CAN Conference CAN in Automation*, CiA publications, Nuremberg, Germany (2008).
13. C. Canudas de Wit et al., "A new model for control of system with friction," *IEEE Trans. Automat. Contr.* **40**(3), 419-425 (1995).
14. B. Armstrong-Helouvy, *Control of Machines with Friction*, Kluwer, New York (1991).
15. A. O'Dwyer, *Handbook of PI and PID Controller Tuning Rules*, 1st ed., Imperial College Press, New York (2001).
16. K. J. Astrom and T. Hagglund, *Advanced PID Control*, Instrumentation Systems and Automation Society, North Carolina (2006).
17. B. W. Leonhard, *Control of Electric Drives*, Springer, New York (2001).
18. T. S. Kumar and R. N. Banavar, "Design and development of telescope control system and software for the 50/80 cm Schmidt telescope," *Proc. SPIE* **8444**, 84445O (2012).



**Tripurari S. Kumar** serves at ARIES Nainital, as an incharge of electronics engineering and works primarily in the Telescope Engineering Group. He is a PI for electronics and software development of the 50/80 cm ARIES Schmidt telescope. He is also a Co-PI for the faint object spectrograph CCD camera development for the 3.6 m ARIES telescope and a member of 3.6 m telescope project. He has worked as an engineer for nearly 11 years spending 9 years in various developmental activities for the ground based observational facilities. He is currently pursuing PhD programme in advanced axes and mirror control techniques for the ground based telescopes at Indian Institute of Technology (IIT) Bombay under the supervision of Prof. Ravi N. Banavar, Systems and Control Engineering. He is one of the members in TMT-India project and engineer coordinator from ARIES for the same.



**Ravi N. Banavar** is currently a professor and convener, Systems and Control Engineering, IIT Bombay. His area of research is optimal control, geometric mechanics and nonlinear control, Lagrangian and Hamiltonian mechanics with area of application in mechanical (robotics), aerospace (launch vehicles, spacecrafts) and electrical power system networks. He has contributed many research publications with recent contributions in the area of geometric mechanics, nonlinear control, power systems applications and other control applications like telescopes, dielectrophoresis and coordination and rendezvous. He did his PhD in 1992 from University of Texas at Austin and joined IIT Bombay in 1993 as a faculty member. In between he was a lecturer at Department of Mechanical and Aerospace Engineering, University of California at Los Angeles. He is an associate editor, Systems and Control Letters and International Journal of Control.